# Modeling the Size-Dependent Nanostructures: Incorporating the Bulk and Surface Effects

Long Zhang, Ph.D.[1]; Binglei Wang[2]; Shenjie Zhou[3]; and Yiguo Xue[4]

**Abstract:** To precisely model the size dependencies in nanostructures, the surface effect and bulk effect are incorporated. From the physical point of view, size dependencies stem from not only the surface, but also the bulk. The surface energy theory and strain gradient elasticity theory are introduced to characterize the surface effect and bulk effect, respectively. The new models for Bernoulli-Euler and Timoshenko beams are developed. Governing equations, initial conditions, and boundary conditions are derived simultaneously by using Hamilton's principle. The new models, incorporating the Poisson effect, contain three material length scale parameters and three surface elasticity constants to capture the size effect in the bulk and surface layer of the beam, respectively. The models recover the models, where either the bulk effect or the surface effect is considered, and also can degenerate into the corresponding modified couple stress models or the classical models when some constants are ignored. In addition, the new Timoshenko beam model recovers the new Bernoulli-Euler beam when shear deformation is ignored. To illustrate the new models, the static bending and free vibration problems of the simply supported nanoscale Bernoulli-Euler and Timoshenko beams are solved, respectively. Numerical results reveal that the differences in the deflection, rotation, and natural frequency predicted by the present model and the other models are large when the beam thickness is small. These differences, however, are decreasing or even diminishing with the increase in the size of the beams. The models may guide the precise design of nanobeam-based devices for a wide range of potential applications. **DOI:** 10.1061/(ASCE)NM.2153-5477.0000117. *© 2016 American Society of Civil Engineers.*

**Author keywords:** Bernoulli-Euler beam; Timoshenko beam; Size effect; Strain gradient theory; Surface elasticity.

## Introduction

Micro/nanostructures such as beams and plates have been widely used in microelectromechanical system (MEMS) and nanoelectromechanical system (NEMS) devices. Numerous experiments have observed the size-dependent behaviors in metals (Poole et al. 1996), brittle materials (Vardoulakis et al. 1998), polymers (Lam and Chong 1999; Lam et al. 2003; McFarland and Colton 2005), and polysilicon (Chasiotis and Knauss 2003; Sadeghian et al. 2011). These behaviors cannot be explained using the classical continuum theory, which has no material length scale parameters. Recently, size-dependent continuum theories have thus received increasing attention in modeling micro/nanostructures and devices, such as nonlocal continuum theory (Eringen 1983), surface energy theory (Gurtin and Murdoch 1975), couple stress theory (Yang et al. 2002), and strain gradient elasticity theory (Lam et al. 2003).

When applying the nonlocal theory (Eringen 1983), a paradoxical conclusion arises: The small length-scale effect vanishes in the bending deflection for the Euler-Bernoulli cantilever nanobeam under a transverse point load (Liang et al. 2015). Moreover, the nonlocal theory predicts a *softening effect*, which is inconsistent with the *stiffening effect* observed in experiments (Lam et al. 2003).

[1]School of Civil Engineering, Shandong Univ., Jinan 250061, China.

[2]Professor, School of Civil Engineering, Shandong Univ., Jinan 250061, China (corresponding author). E-mail: bwang@sdu.edu.cn

[3]Professor, School of Mechanical Engineering, Shandong Univ., Jinan 250061, China.

[4]Professor, Research Center of Geotechnical and Structural Engineering, Shandong Univ., Jinan 250061, China.

Note. This manuscript was submitted on January 7, 2016; approved on October 7, 2016; published online on November 30, 2016. Discussion period open until April 30, 2017; separate discussions must be submitted for individual papers. This paper is part of the ***Journal of Nanomechanics and Micromechanics***, © ASCE, ISSN 2153-5434.

For surface energy theory, it is considered that the surface properties cannot be overlooked in the study of nanostructures and nanomaterials due to the large value of surface area to volume ratios in nanoscale structures (Gurtin and Murdoch 1975). A number of works have been conducted to study the size-dependent behaviors in nanostructures (Jiang and Yan 2010; Koochi et al. 2013). With surface energy effects considered, the general Euler-Bernoulli and Timoshenko models based on the Gurtin–Murdoch continuum theory were presented to analyze thick and thin nanoscale beams with an arbitrary cross section (Chang and Rajapakse 2010). Gao's group also proposed beam and plate models with microstructure and surface energy to study the size-dependent mechanical properties (Gao 2015; Gao and Mahmoud 2014; Shaat et al. 2014).

The couple stress theory is a nonclassical continuum theory in which higher-order stresses, known as the couple stresses (Koiter 1964) exist. Afterward, Yang et al. (2002) modified the classical couple stress theory and proposed a modified couple stress theory involving only one additional material length scale parameter (MLSP). Since then, numerous works have emerged and been developed to study the size effect of the linear and nonlinear Bernoulli–Euler beam (Fathalilou et al. 2014; Park and Gao 2006; Xia et al. 2010), the linear and nonlinear Timoshenko beam (Asghari et al. 2010b; Ma et al. 2008), the linear functionally graded Euler-Bernoulli beam (Asghari et al. 2010a), the Timoshenko beam (Asghari et al. 2011), the Kirchhoff plate (Tsiatas 2009), and pull-in phenomena in MEMS (Yin et al. 2011).

The strain gradient elasticity theory (Lam et al. 2003), which can reduce to the modified couple stress theory (Yang et al. 2002) previously mentioned, introduces three MLSPs to capture the size effects. In other words, the strain gradient elasticity theory is a more general theory than the modified couple stress theory as the authors' previous work has pointed out (Wang et al. 2010). Strain gradient elasticity theory has been applied to study the linear

(Kong et al. 2009) and nonlinear (Zhao et al. 2012) Euler beam, linear (Wang et al. 2010) and nonlinear (Asghari et al. 2010b) Timoshenko beam, and Reddy-Levinson beam (Wang et al. 2014), and is also employed to investigate the size-dependent pull-in phenomena in MEMS (Liang et al. 2015; Wang et al. 2011c, 2012).

The modified couple stress theory only introduces symmetric rotation gradient tensor, resulting in one length scale. While the strain gradient theory introduces not only the symmetric rotation gradient tensor but also the dilatation gradient tensor and the deviatoric stretch gradient tensor, resulting in three length scales. These length scales are internal parameters for a given material and should be determined from experiments with different sizes, e.g., axial, uniaxial, tensile or compressive, torsional, or bending experiments. The strain gradient theory can degenerate into the modified couple stress theory. That is, the modified couple stress theory is a special case of the strain gradient theory. Compared with the modified couple stress theory, the strain gradient theory is more versatile.

It is noted that the surface energy theory characterizes the size effect, considering only the effect of the surface layer; and the modified couples stress theory and strain gradient theory characterize the size effect, considering only the effect of the bulk material. In other words, these theories characterize the size effect either from the bulk part or from the surface part: the surface energy theory is the former, while the modified couple stress theory and strain gradient theory are the latter. In the current literatures, size effect in miniaturized structures has been studied either from the point of the bulk or from the surface, why not from both? Although these theories are widely applied to study the size-dependent behaviors individually, one has to admit that the mechanical properties are not only relative to the surface part but also relative to the bulk part because the characteristic length is in the bulk, such as the grain size or atomic lattice spacing. In literature, almost all the works characterize the size effect either from the surface or from the bulk (Wang et al. 2010, 2011a). Few works are carried out to study the size effect with both effects included (Gao 2015; Gao and Mahmoud 2014). The couple stress theory introduces only one MLSP, while the strain gradient theory introduces three MLSPs. Compared with the couple stress theory, the strain gradient theory is versatile. But no work has been developed to study the size effect based on the surface energy theory and strain gradient theory.

The paper aims to close the aforementioned gap by establishing versatile size-dependent beam models incorporating the surface and bulk effect. The rest of the paper is organized as follows. In section "Formulation," the variational formulations of the nanoscale Bernoulli-Euler and Timoshenko beams based on the strain gradient elasticity theory and surface energy theory are in detail deduced by using the Hamilton's principle. Then governing equations, initial conditions, and all possible boundary conditions are obtained simultaneously. Subsequently, the static bending and free vibration problems for the simply supported Bernoulli-Euler and Timoshenko beams are solved respectively, and the corresponding numerical results for both problems are analyzed and discussed in section "Case Study for a Simply Supported Nanobeam." Finally, some major conclusions are summarized in section "Conclusions."

## Formulation

According to the strain gradient theory proposed by Lam et al. (2003), the strain energy $U_B$ in a deformed isotropic linear elastic material occupying region $\Omega$ is written as

$$U_B = \frac{1}{2}\int_{\Omega}(\sigma_{ij}\varepsilon_{ij} + p_i\gamma_i + \tau^{(1)}_{ijk}\eta^{(1)}_{ijk} + m^s_{ij}\chi^s_{ij})dV \tag{1}$$

where

$$\varepsilon_{ij} = \frac{1}{2}(u_{i,j} + u_{j,i}) \tag{2}$$

$$\gamma_i = \varepsilon_{mm,i} \tag{3}$$

$$\eta^{(1)}_{ijk} = \eta^s_{ijk} - \frac{1}{5}(\delta_{ij}\eta^s_{mmk} + \delta_{jk}\eta^s_{mmi} + \delta_{ki}\eta^s_{mmj}) \tag{4}$$

$$\chi^s_{ij} = \frac{1}{2}(e_{ipq}\varepsilon_{qj,p} + e_{jpq}\varepsilon_{qi,p}) \tag{5}$$

where $\varepsilon_{ij}$ = strain tensor; $\gamma_i$ = dilatation gradient tensor; $\eta^{(1)}_{ijk}$ = deviatoric stretch gradient tensor; $\chi^s_{ij}$ = symmetric rotation gradient tensor; $u_i$ = displacement vector; $\varepsilon_{mm}$ = dilatation strain tensor; $\delta_{ij}$, and $e_{ijk}$ are the Knocker symbol and the alternate symbol, respectively; and $\eta^s_{ijk}$ = symmetric part of second-order displacement gradient tensor, given by

$$\eta^s_{ijk} = \frac{1}{3}(u_{i,jk} + u_{j,ki} + u_{k,ij}) \tag{6}$$

In the subsequent equations, unless otherwise stated, the index notation will be used with repeated indices denoting summation from 1 to 3.

And the corresponding stress measures are respectively given as

$$\sigma_{ij} = \lambda\delta_{ij}\varepsilon_{mm} + 2\mu\varepsilon_{ij} \tag{7}$$

$$p_i = 2\mu l_0^2\gamma_i \tag{8}$$

$$\tau^{(1)}_{ijk} = 2\mu l_1^2\eta^{(1)}_{ijk} \tag{9}$$

$$m^s_{ij} = 2\mu l_2^2\chi^s_{ij} \tag{10}$$

where $l_0$, $l_1$, $l_2$ = additional independent MLSPs associated with the dilatation gradients, deviatoric stretch gradients, and symmetric rotation gradients, respectively. The parameters $\lambda$ and $\mu$ in the constitutive equation of the classical stress $\sigma_{ij}$ are Lamé constants. They can be written in terms of the Young modulus $E$ and the Poisson's ratio $v$ as

$$\lambda = \frac{Ev}{(1+v)(1-2v)}, \qquad \mu = \frac{E}{2(1+v)} \tag{11}$$

On the other hand, based on the surface elasticity theory (Gurtin and Murdoch 1978), the in-plane components of the surface stress tensor $\tau_{\alpha\beta}$ are given by

$$\tau_{\alpha\beta} = [\tau_0 + (\lambda_0 + \tau_0)u_{\gamma,\gamma}]\delta_{\alpha\beta} + \mu_0(u_{\alpha,\beta} + u_{\beta,\alpha}) - \tau_0 u_{\beta,\alpha} \tag{12}$$

where $\tau_0$ = residual surface stress (i.e., the surface stress at zero strain), and $\mu_0$ and $\lambda_0$ are the surface elastic constants, which can be determined by atomistic simulations (Shenoy 2005). Obviously, Eq. (12) shows that $\tau_{\alpha\beta}$ is not symmetric.

The out-plane components of the surface stress tensor are given by (Gurtin and Murdoch 1978)

$$\tau_{n\alpha} = \tau_0 u_{n,\alpha} \tag{13}$$

where $n$ = direction of the outward unit normal $n$ on the surface.

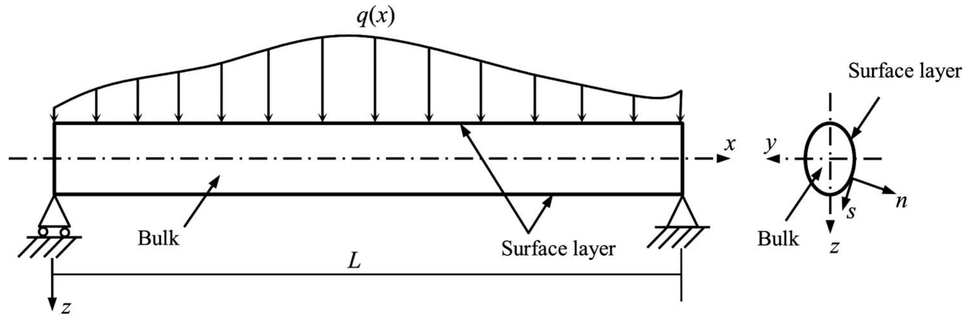


**Fig. 1.** Schematic of a nanobeam with surface layer



### *Model of the Bernoulli-Euler Nanobeam*

Consider a straight Bernoulli-Euler beam subjected to a static lateral load $q(x)$, as shown in Fig. 1, in which the loading plane coincides with the $x$-$z$ plane, and the cross section of the beam parallels to the $y$-$z$ plane. As shown in Fig. 1, the beam is considered to have an elastic surface (mathematically zero thickness) perfectly bonded to its bulk material. The surface layer has distinct material properties and accounts for the surface energy effects (Gurtin and Murdoch 1975, 1978).

According to the Bernoulli-Euler hypothesis, the displace field of the beam can be expressed as

$$u_1(x,y,z,t) = -z\frac{\partial w(x,t)}{\partial x}, \qquad u_2(x,y,z,t) = 0,$$
$$u_3(x,y,z,t) = w(x,t) \tag{14}$$

Using Eqs. (2) and (14), the nonzero strain $\varepsilon_{ij}$ can be obtained as

$$\varepsilon_{11} = -z\frac{\partial^2 w}{\partial x^2} \tag{15}$$

Substituting Eq. (15) into Eq. (3), it then follows that

$$\gamma_1 = -z\frac{\partial^3 w}{\partial x^3}, \qquad \gamma_3 = -\frac{\partial^2 w}{\partial x^2} \tag{16}$$

From Eqs. (5) and (15), it leads to

$$\chi_{12}^s = \chi_{21}^s = -\frac{1}{2}\frac{\partial^2 w}{\partial x^2} \tag{17}$$

By using Eqs. (4), (6), and (14), it leads to

$$\eta_{111}^{(1)} = -\frac{2}{5}z\frac{\partial^3 w}{\partial x^3}, \qquad \eta_{333}^{(1)} = \frac{1}{5}\frac{\partial^2 w}{\partial x^2},$$
$$\eta_{113}^{(1)} = \eta_{311}^{(1)} = \eta_{131}^{(1)} = -\frac{4}{15}\frac{\partial^2 w}{\partial x^2}$$
$$\eta_{221}^{(1)} = \eta_{122}^{(1)} = \eta_{212}^{(1)} = \eta_{331}^{(1)} = \eta_{133}^{(1)} = \eta_{313}^{(1)} = \frac{1}{5}z\frac{\partial^3 w}{\partial x^3}$$
$$\eta_{223}^{(1)} = \eta_{322}^{(1)} = \eta_{232}^{(1)} = \frac{1}{15}\frac{\partial^2 w}{\partial x^2} \tag{18}$$

By substituting Eq. (15) into Eq. (7), the nonzero components of stresses $\sigma_{ij}$ can be achieved

$$\sigma_{11} = -(\lambda+2\mu)z\frac{\partial^2 w}{\partial x^2}, \qquad \sigma_{22} = \sigma_{33} = -\lambda z\frac{\partial^2 w}{\partial x^2} \tag{19}$$

By using Eqs. (8)–(10) and (16)–(18), the nonzero components of the stress measures $p_i$, $m_{ij}^s$, and $\tau_{ijk}^{(1)}$ are respectively

$$p_1 = -2\mu l_0^2 z\frac{\partial^3 w}{\partial x^3}, \qquad p_3 = -2\mu l_0^2\frac{\partial^2 w}{\partial x^2} \tag{20}$$

$$m_{12}^s = m_{21}^s = -\mu l_2^2\frac{\partial^2 w}{\partial x^2} \tag{21}$$

$$\tau_{111}^{(1)} = -\frac{4}{5}\mu l_1^2 z\frac{\partial^3 w}{\partial x^3}, \qquad \tau_{333}^{(1)} = \frac{2}{5}\mu l_1^2\frac{\partial^2 w}{\partial x^2}$$
$$\tau_{113}^{(1)} = \tau_{311}^{(1)} = \tau_{131}^{(1)} = -\frac{8}{15}\mu l_1^2\frac{\partial^2 w}{\partial x^2}$$
$$\tau_{221}^{(1)} = \tau_{122}^{(1)} = \tau_{212}^{(1)} = \tau_{331}^{(1)} = \tau_{133}^{(1)} = \tau_{313}^{(1)} = \frac{2}{5}\mu l_1^2 z\frac{\partial^3 w}{\partial x^3}$$
$$\tau_{223}^{(1)} = \tau_{322}^{(1)} = \tau_{232}^{(1)} = \frac{2}{15}\mu l_1^2\frac{\partial^2 w}{\partial x^2} \tag{22}$$

From Eqs. (12)–(14), it follows that

$$\tau_{xx} = \tau_0 - (\lambda_0 + 2\mu_0)z\frac{\partial^2 w}{\partial x^2}, \qquad \tau_{nx} = \tau_0 n_z\frac{\partial w}{\partial x} \tag{23}$$

where $n_z = z$-component of the unit outward normal vector $n$ to the beam lateral surface.

The total strain energy in the elastically deformed beam is given by

$$U_T = U_B + U_S = \frac{1}{2}\int_0^L \iint_A (\sigma_{ij}\varepsilon_{ij} + p_i\gamma_i + \tau_{ijk}^{(1)}\eta_{ijk}^{(1)} + m_{ij}^s\chi_{ij}^s)$$
$$\times\, dAdx + \frac{1}{2}\int_0^L \oint_{\partial A}\tau_{ij}\varepsilon_{ij}dsdx \tag{24}$$

where $U_B$ = strain energy in the bulk of the beam based on the strain gradient elasticity theory; and $U_S$ = strain energy in the surface layer based on the surface elasticity theory. $L$ = length of the beam, $A$ = cross-sectional area of the beam, and $\partial A$ = boundary of $A$.

By using Eqs. (15)–(24), the first variation of the total strain energy in the beam in the time interval $[0,T]$ can be determined as [the superscript $(i)$ denotes $i$th differentiation with respect to $x$]

$$\begin{aligned}\delta U_T &= \delta U_B + \delta U_S\\ &= \int_0^T\int_0^L [Sw^{(4)} + (\lambda_0+2\mu_0)I_P w^{(4)} - Kw^{(6)} - \tau_0 S_P w'']\delta w dxdt\\ &\quad + \int_0^T [-Sw^{(3)} + Kw^{(5)} - (\lambda_0+2\mu_0)I_P w^{(3)} + \tau_0 S_P w']\delta w|_0^L dt\\ &\quad + \int_0^T \left[Sw'' - Kw^{(4)} + (\lambda_0+2\mu_0)I_P w'' - \frac{1}{2}\tau_0 P_A\right]\delta w'|_0^L dt\\ &\quad + \int_0^T Kw^{(3)}\delta w''|_0^L dt\end{aligned} \tag{25}$$

where

$$K = I(2\mu l_0^2 + \frac{4}{5}\mu l_1^2),$$
$$S = (\lambda + 2\mu)I + 2\mu l_0^2 A + \frac{8}{15}\mu l_1^2 A + \mu l_2^2 A \tag{26}$$

in which

$$I = \int_A z^2 dA \tag{27}$$

and $S_P$ is defined as

$$S_P = \oint_{\partial A} n_z^2 ds \tag{28}$$

and $P_A$, $I_P$ are the first and second moment of beam cross-sectional perimeter, respectively, defined by

$$P_A = \oint_{\partial A} z ds \tag{29}$$

$$I_P = \oint_{\partial A} z^2 ds \tag{30}$$

The first variation of the work can be written as

$$\delta W = \int_0^L q\delta w dx + V\delta w|_0^L + M\delta w'|_0^L + M^h \delta w''|_0^L \tag{31}$$

where $q$ = external force, $V$ = boundary shear force, $M$ and $M^h$ are the boundary classical and nonclassical moments, respectively.

The first variation of the kinetic energy of the beam, in the time interval $[0, T]$, can be determined to be

$$\int_0^T \delta T dt = \delta \int_0^T \int_V \frac{1}{2}\rho\left(\frac{\partial w}{\partial t}\right)^2 dV dt$$
$$= \int_0^T \int_0^L (-m_0 \ddot{w} \delta w) dx dt + \int_0^L (m_0 \dot{w} \delta w)|_{t=0}^{t=T} dx \tag{32}$$

where

$$m_0 = \rho A, \qquad \ddot{w} = \frac{\partial^2 w}{\partial t^2}, \qquad \dot{w} = \frac{\partial w}{\partial t} \tag{33}$$

It is noted that some works (e.g., Kong et al. 2009) ignored the kinetic energy corresponding to the velocity of $u_1$, so it is not considered here.

According to Hamilton's principle

$$\delta \int_{t_1}^{t_2} [T - (U_T - W)] dt = 0 \tag{34}$$

by substituting Eqs. (25), (31), and (32) into Eq. (34), it then leads to

$$\begin{aligned}
&\int_0^T \int_0^L [S w^{(4)} + (\lambda_0 + 2\mu_0) I_P w^{(4)} - K w^{(6)} - \tau_0 S_P w'' + m_0 \ddot{w} - q] \delta w dx dt \\
&+ \int_0^T [-S w^{(3)} + K w^{(5)} - (\lambda_0 + 2\mu_0) I_P w^{(3)} + \tau_0 S_P w' - V] \delta w|_0^L dt \\
&+ \int_0^T \left[S w'' - K w^{(4)} + (\lambda_0 + 2\mu_0) I_P w'' - \frac{1}{2}\tau_0 P_A - M\right] \delta w'|_0^L dt \\
&+ \int_0^T [K w^{(3)} - M^h] \delta w''|_0^L dt + \int_0^L \left(m_0 \frac{\partial w}{\partial t} \delta w\right)|_{t=0}^{t=T} dx = 0
\end{aligned} \tag{35}$$

The preceding variation equation implies that each term must be equal to zero, so the governing equation of the beam is given by

$$S w^{(4)} + (\lambda_0 + 2\mu_0) I_P w^{(4)} - K w^{(6)} - \tau_0 S_P w'' + m_0 \ddot{w} - q = 0 \tag{36}$$

The boundary conditions can be written as

$$\begin{aligned}
&[-S w^{(3)} + K w^{(5)} - (\lambda_0 + 2\mu_0) I_P w^{(3)} + \tau_0 S_P w' - V]|_0^L = 0 \quad \text{or} \quad w = \bar{w} \quad \text{at } x = 0 \quad \text{and} \quad x = L \\
&\left[S w'' - K w^{(4)} + (\lambda_0 + 2\mu_0) I_P w'' - \frac{1}{2}\tau_0 P_A - M\right]\Bigg|_0^L = 0 \quad \text{or} \quad w' = \bar{w}' \quad \text{at } x = 0 \quad \text{and} \quad x = L \\
&[K w^{(3)} - M^h]|_0^L = 0 \quad \text{or} \quad w'' = \bar{w}'' \quad \text{at } x = 0 \quad \text{and} \quad x = L
\end{aligned} \tag{37}$$

where the overbar represents the prescribed value.

And the initial conditions can be written as

$$(m_0 \dot{w} \delta w)|_{t=0}^{t=T} = 0 \tag{38}$$

### *Model of the Timoshenko Nanobeam*

Consider a straight Timoshenko beam, which is subjected to distributed loads $q$, $f_u$, and $f_\phi$ through the longitudinal axis $x$ of the beam, as shown in Fig. 1, in which the loading plane coincides with the $x$-$z$ plane, and the cross section of the beam parallels to the $y$-$z$ plane. As shown in Fig. 1, the beam also is considered to have an elastic surface (mathematically zero thickness) perfectly bonded to its bulk material. The surface layer has distinct material properties and accounts for the surface energy effects.

The displacement fields based on the Timoshenko beam theory can be given by (Dym and Shames 1973)

$$u_1(x,y,z,t) = u(x,t) - z\phi(x,t), \qquad u_2(x,y,z,t) = 0,$$
$$u_3(x,y,z,t) = w(x,t) \tag{39}$$

By using Eqs. (2) and (39), the nonzero components of strain tensor are

$$\varepsilon_{11} = \frac{\partial u}{\partial x} - z\frac{\partial \phi}{\partial x}, \qquad \varepsilon_{13} = \varepsilon_{31} = \frac{1}{2}\left(\frac{\partial w}{\partial x} - \phi\right) \tag{40}$$

Substituting Eq. (40) into Eq. (3) then leads to

$$\gamma_1 = \frac{\partial^2 u}{\partial x^2} - z\frac{\partial^2 \phi}{\partial x^2}, \qquad \gamma_3 = -\frac{\partial \phi}{\partial x} \tag{41}$$

From Eqs. (5) and (40), it follows that

$$\chi^s_{12} = \chi^s_{21} = -\frac{1}{4}\left(\frac{\partial^2 w}{\partial x^2} + \frac{\partial \phi}{\partial x}\right) \tag{42}$$

By using Eqs. (4), (6), and (39), it follows that

$$\eta^{(1)}_{111} = \frac{2}{5}\left(\frac{\partial^2 u}{\partial x^2} - z\frac{\partial^2 \phi}{\partial x^2}\right), \qquad \eta^{(1)}_{333} = -\frac{1}{5}\left(\frac{\partial^2 w}{\partial x^2} - 2\frac{\partial \phi}{\partial x}\right)$$

$$\eta^{(1)}_{113} = \eta^{(1)}_{311} = \eta^{(1)}_{131} = \frac{4}{15}\left(\frac{\partial^2 w}{\partial x^2} - 2\frac{\partial \phi}{\partial x}\right)$$

$$\eta^{(1)}_{221} = \eta^{(1)}_{122} = \eta^{(1)}_{212} = \eta^{(1)}_{331} = \eta^{(1)}_{133} = \eta^{(1)}_{313} = -\frac{1}{5}\left(\frac{\partial^2 u}{\partial x^2} - z\frac{\partial^2 \phi}{\partial x^2}\right)$$

$$\eta^{(1)}_{223} = \eta^{(1)}_{322} = \eta^{(1)}_{232} = -\frac{1}{15}\left(\frac{\partial^2 w}{\partial x^2} - 2\frac{\partial \phi}{\partial x}\right) \tag{43}$$

By substituting Eq. (40) into Eq. (7), the nonzero components of stresses $\sigma_{ij}$ can be achieved

$$\sigma_{11} = (\lambda + 2\mu)\left(\frac{\partial u}{\partial x} - z\frac{\partial \phi}{\partial x}\right), \qquad \sigma_{22} = \sigma_{33} = \lambda\left(\frac{\partial u}{\partial x} - z\frac{\partial \phi}{\partial x}\right),$$

$$\sigma_{13} = \sigma_{31} = \mu\left(\frac{\partial w}{\partial x} - \phi\right) \tag{44}$$

It is worth noting that the variation of $\sigma_{13}$ and $\sigma_{31}$ depends only on $x$. In order to take the nonuniformity of the shear strain into account over the beam cross section, a correction factor $k_s$, which depends on the shape of the beam cross section, is introduced to the stress component $\sigma_{13}$ and $\sigma_{31}$ as follows:

$$\sigma_{13} = \sigma_{31} = k_s\mu\left(\frac{\partial w}{\partial x} - \phi\right) \tag{45}$$

By using Eqs. (8)–(10) and (41)–(43), the nonzero components of the stress measures $p_i$, $m^s_{ij}$, and $\tau^{(1)}_{ijk}$ are, respectively

$$p_1 = 2\mu l_0^2\left(\frac{\partial^2 u}{\partial x^2} - z\frac{\partial^2 \phi}{\partial x^2}\right), \qquad p_3 = -2\mu l_0^2\frac{\partial \phi}{\partial x} \tag{46}$$

$$m^s_{12} = m^s_{21} = -\frac{1}{2}\mu l_2^2\left(\frac{\partial^2 w}{\partial x^2} + \frac{\partial \phi}{\partial x}\right) \tag{47}$$

$$\tau^{(1)}_{111} = \frac{4}{5}\mu l_1^2\left(\frac{\partial^2 u}{\partial x^2} - z\frac{\partial^2 \phi}{\partial x^2}\right), \qquad \tau^{(1)}_{333} = -\frac{2}{5}\mu l_1^2\left(\frac{\partial^2 w}{\partial x^2} - 2\frac{\partial \phi}{\partial x}\right)$$

$$\tau^{(1)}_{113} = \tau^{(1)}_{311} = \tau^{(1)}_{131} = \frac{8}{15}\mu l_1^2\left(\frac{\partial^2 w}{\partial x^2} - 2\frac{\partial \phi}{\partial x}\right)$$

$$\tau^{(1)}_{221} = \tau^{(1)}_{122} = \tau^{(1)}_{212} = \tau^{(1)}_{331} = \tau^{(1)}_{133} = \tau^{(1)}_{313} = -\frac{2}{5}\mu l_1^2\left(\frac{\partial^2 u}{\partial x^2} - z\frac{\partial^2 \phi}{\partial x^2}\right)$$

$$\tau^{(1)}_{223} = \tau^{(1)}_{322} = \tau^{(1)}_{232} = -\frac{2}{15}\mu l_1^2\left(\frac{\partial^2 w}{\partial x^2} - 2\frac{\partial \phi}{\partial x}\right) \tag{48}$$

From Eqs. (12), (13), and (39), it follows that, with $\alpha, \beta \in \{x, s\}$ on the beam lateral surface

$$\tau_{xx} = \tau_0 + (\lambda_0 + 2\mu_0)\left(\frac{\partial u}{\partial x} - z\frac{\partial \phi}{\partial x}\right),$$

$$\tau_{xs} = \left[(\mu_0 - \tau_0)\frac{\partial w}{\partial x} - \mu_0\phi\right]n_y \equiv \tau_{xz}n_y$$

$$\tau_{sx} = \left[\mu_0\frac{\partial w}{\partial x} - (\mu_0 - \tau_0)\phi\right]n_y \equiv \tau_{xz}n_y,$$

$$\tau_{nx} = \tau_0 n_z\frac{\partial w}{\partial x} \tag{49}$$

where $n_y$ and $n_z$ = $y$- and $z$-components of the unit outward normal vector $n$ to the beam lateral surface, respectively (i.e., $n_y = \cos\theta$ and $n_z = \sin\theta$). In addition, $\theta$ = angle between the $y$-axis and the normal vector $n$, which is shown in Fig. 1, and $s$ denotes the direction of the unit tangent vector $s$ on the boundary of the beam cross section. When $\theta = 0$, $\tau_{xz}$ and $\tau_{zx}$ = the values of $\tau_{xs}$ and $\tau_{sx}$, respectively.

The total strain energy in the elastically deformed beam is given by

$$U_T = U_B + U_S = \frac{1}{2}\int_0^L \iint_A (\sigma_{ij}\varepsilon_{ij} + p_i\gamma_i + \tau^{(1)}_{ijk}\eta^{(1)}_{ijk} + m^s_{ij}\chi^s_{ij}) \times dAdx + \frac{1}{2}\int_0^L \oint_{\partial A}\tau_{ij}\varepsilon_{ij}dsdx \tag{50}$$

where $U_B$ = strain energy in the bulk of the beam based on the strain gradient elasticity theory; and $U_S$ = strain energy in the surface layer based on the surface elasticity theory. $L$ = length of the beam, $A$ = cross-sectional area of the beam, and $\partial A$ = boundary of $A$.

By using Eqs. (40)–(50), the total strain energy is

$$\begin{aligned} U_T = U_B + U_S &= \frac{1}{2}\int_0^L \iint_A (\sigma_{ij}\varepsilon_{ij} + p_i\gamma_i + \tau^{(1)}_{ijk}\eta^{(1)}_{ijk} + m^s_{ij}\chi^s_{ij})dAdx + \frac{1}{2}\int_0^L \oint_{\partial A}\tau_{ij}\varepsilon_{ij}dsdx \\ &= \frac{1}{2}\int_0^L \iint_A (\sigma_{11}\varepsilon_{11} + 2\sigma_{13}\varepsilon_{13} + p_1\gamma_1 + p_3\gamma_3 + \tau^{(1)}_{111}\eta^{(1)}_{111} + \tau^{(1)}_{333}\eta^{(1)}_{333} + 3\tau^{(1)}_{113}\eta^{(1)}_{113} + 3\tau^{(1)}_{223}\eta^{(1)}_{223} + 6\tau^{(1)}_{221}\eta^{(1)}_{221} + 2m^s_{12}\chi^s_{12})dAdx \\ &\quad + \frac{1}{2}\int_0^L \oint_{\partial A}(\tau_{xx}\varepsilon_{xx} + \tau_{xs}\varepsilon_{xs} + \tau_{sx}\varepsilon_{sx} + 2\tau_{nx}\varepsilon_{nx})dsdx \end{aligned} \tag{51}$$

where

$$\varepsilon_{sx} = \frac{1}{2}\left(-\phi + \frac{\partial w}{\partial x}\right)n_y = \varepsilon_{xs}, \qquad \varepsilon_{nx} = \frac{1}{2}\frac{\partial w}{\partial x}n_z = \varepsilon_{xn} \tag{52}$$

By using Eqs. (40)–(52), the first variation of the total strain energy in the beam in the time interval $[0,T]$ can be determined as follows [with the superscript $(i)$ denoting the $i$th differentiation with respect to $x$]:

$$\delta\int_0^T U_T dt = \delta\int_0^T (U_B+U_S)dt = \int_0^T\int_0^L (f_{(u)}\delta u + f_{(w)}\delta w + f_{(\phi)}\delta\phi)dxdt + \int_0^T\left(k_2u' - k_1u^{(3)} + N_s - \frac{1}{2}\tau_0 C_p\right)\delta u|_{x=0}^{x=L}dt$$
$$+\int_0^T k_1u''\delta u'|_{x=0}^{x=L}dt + \int_0^T\left(-k_7w^{(3)} + k_5w' + k_6\phi'' - k_5\phi + \frac{1}{2}Q_{s1} + \frac{1}{2}Q_{s2} + \tau_0 S_P w'\right)\delta w|_{x=0}^{x=L}dt$$
$$+\int_0^T (k_7w'' - k_6\phi')\delta w'|_{x=0}^{x=L}dt + \int_0^T\left(k_4\phi' - k_6w'' - k_3\phi^{(3)} - M_s + \frac{1}{2}\tau_0 P_A\right)\delta\phi|_{x=0}^{x=L}dt + \int_0^T k_3\delta\phi'|_{x=0}^{x=L}dt \quad (53)$$

where

$$f_{(u)} = k_1u^{(4)} - k_2u'' - \frac{\partial N_s}{\partial x}$$
$$f_{(w)} = k_7w^{(4)} - k_6\phi^{(3)} + k_5(-w''+\phi') - \frac{1}{2}\frac{\partial Q_{s1}}{\partial x} - \frac{1}{2}\frac{\partial Q_{s2}}{\partial x} - \tau_0 S_P w''$$
$$f_{(\phi)} = k_3\phi^{(4)} + k_6w^{(3)} - k_4\phi'' + k_5(-w'+\phi) + \frac{\partial M_s}{\partial x} - \frac{1}{2}Q_{s1} - \frac{1}{2}Q_{s2} \quad (54)$$

and

$$k_1 = \mu A\left(2l_0^2 + \frac{4}{5}l_1^2\right), \qquad k_2 = A(\lambda+2\mu), \qquad k_3 = \mu I\left(2l_0^2 + \frac{4}{5}l_1^2\right)$$
$$k_4 = \left[\mu A\left(2l_0^2 + \frac{32}{15}l_1^2 + \frac{1}{4}l_2^2\right) + I(\lambda+2\mu)\right], \qquad k_5 = k_s\mu A$$
$$k_6 = \mu A\left(\frac{16}{15}l_1^2 - \frac{1}{4}l_2^2\right), \qquad k_7 = \mu A\left(\frac{8}{15}l_1^2 + \frac{1}{4}l_2^2\right) \quad (55)$$

where

$$I = \int_A z^2 dA \quad (56)$$

and

$$N_s \equiv \oint_{\partial A}\tau_{xx}ds, \qquad M_s \equiv \oint_{\partial A}\tau_{xx}zds, \qquad Q_{s1} \equiv \oint_{\partial A}\tau_{xz}n_y^2ds, \qquad Q_{s2} \equiv \oint_{\partial A}\tau_{zx}n_y^2ds \quad (57)$$

and

$$S_P \equiv \oint_{\partial A}n_z^2ds, \qquad C_P \equiv \oint_{\partial A}ds, \qquad P_A \equiv \oint_{\partial A}zds \quad (58)$$

From Eqs. (49), (57), and (58), it leads to

$$N_s = \left[\tau_0 + (\lambda_0+2\mu_0)\frac{\partial u}{\partial x}\right]C_P - (\lambda_0+2\mu_0)P_A\frac{\partial\phi}{\partial x}$$
$$M_s = \left[\tau_0 + (\lambda_0+2\mu_0)\frac{\partial u}{\partial x}\right]P_A - (\lambda_0+2\mu_0)I_P\frac{\partial\phi}{\partial x}$$
$$Q_{s1} = \left[(\mu_0-\tau_0)\frac{\partial w}{\partial x} - \mu_0\phi\right]T_p, \qquad Q_{s2} = \left[\mu_0\frac{\partial w}{\partial x} - (\mu_0-\tau_0)\phi\right]T_p \quad (59)$$

where

$$I_P = \oint_{\partial A}z^2ds, \qquad T_P = \oint_{\partial A}n_y^2ds \quad (60)$$

The first variation of the kinetic energy of the beam, in the time interval $[0,T]$ can be determined to be

$$\int_0^T \delta T dt = \delta\int_0^T\int_V \frac{1}{2}\rho\left[\left(\frac{\partial u_1}{\partial t}\right)^2 + \left(\frac{\partial u_2}{\partial t}\right)^2 + \left(\frac{\partial u_3}{\partial t}\right)^2\right]dVdt$$
$$= -\int_0^T\int_0^L\left(m_0\frac{\partial^2 u}{\partial t^2}\delta u + m_0\frac{\partial^2 w}{\partial t^2}\delta w + m_2\frac{\partial^2\phi}{\partial t^2}\delta\phi\right)dxdt + \int_0^L\left(m_0\frac{\partial u}{\partial t}\delta u + m_0\frac{\partial w}{\partial t}\delta w + m_2\frac{\partial\phi}{\partial t}\delta\phi\right)\Bigg|_{t=0}^{t=T}dx \quad (61)$$

where

$$m_0 = \rho A, \qquad m_2 = \rho I \tag{62}$$

The first variations of the work done by the forces applied on the beam in the time interval $[0, T]$ can be expressed as

$$\delta \int_0^T W dt = \int_0^T \int_0^L (f_u \delta u + q\delta w + f_\phi \delta\phi) dx dt + \int_0^T (N_u^0 \delta u + N_u^1 \delta u' + N_w^0 \delta w + N_w^1 \delta w' + N_\phi^0 \delta\phi + N_\phi^1 \delta\phi')|_{x=0}^{x=L} dt \tag{63}$$

where $f_u$ and $q$ are the $x$- and $z$-components of the body forces per unit length, respectively; and $f_\phi$ = body couple per unit length. $N_u^0, N_u^1, N_w^0, N_w^1, N_\phi^0, N_\phi^1$ are external forces work conjugate to $\delta u, \delta u', \delta w, \delta w', \delta\phi, \delta\phi'$, respectively

According to Hamilton's principle

$$\delta \int_{t_1}^{t_2} [T - (U_T - W)] dt = 0 \tag{64}$$

By using Eqs. (53), (61), (63), and (64), it can be achieved

$$\begin{aligned}
&\int_0^T \int_0^L \left[\left(f_u - f_{(u)} - m_0 \frac{\partial^2 u}{\partial t^2}\right)\delta u + \left(q - f_{(w)} - m_0 \frac{\partial^2 w}{\partial t^2}\right)\delta w + \left(f_\phi - f_{(\phi)} - m_2 \frac{\partial^2 \phi}{\partial t^2}\right)\delta\phi\right] dx dt \\
&- \int_0^T \left[\left(k_2 u' - k_1 u^{(3)} + N_s - \frac{1}{2}\tau_0 C_p - N_u^0\right)\delta u + (k_1 u'' - N_u^1)\delta u' + \left(k_4 \phi' - k_6 w'' - k_3 \phi^{(3)} - M_s + \frac{1}{2}\tau_0 P_A - N_\phi^0\right)\delta\phi \right.\\
&\left. + (k_3 - N_\phi^1)\delta\phi' + \left(\frac{1}{2}Q_{s1} + \frac{1}{2}Q_{s2} + \tau_0 S_P w' - N_w^0\right)\delta w + (k_7 w'' - k_6 \phi' - N_w^1)\delta w'\right]\Bigg|_{x=0}^{x=L} dt \\
&+ \int_0^L \left(m_0 \frac{\partial u}{\partial t}\delta u + m_0 \frac{\partial w}{\partial t}\delta w + m_2 \frac{\partial \phi}{\partial t}\delta\phi\right)\Bigg|_{t=0}^{t=T} dx = 0
\end{aligned} \tag{65}$$

Due to the variation, Eq. (65) implies that each term must be equal to zero, it then leads to

$$f_{(u)} = f_u - m_0 \frac{\partial^2 u}{\partial t^2}, \qquad f_{(w)} = q - m_0 \frac{\partial^2 w}{\partial t^2}, \qquad f_{(\phi)} = f_\phi - m_2 \frac{\partial^2 \phi}{\partial t^2} \tag{66}$$

By substituting Eq. (54) into Eq. (66), the governing equations of the beam are given by

$$\begin{aligned}
&k_1 u^{(4)} - [k_2 + (\lambda_0 + 2\mu_0) C_P] u'' + (\lambda_0 + 2\mu_0) P_A \phi'' = f_u - m_0 \frac{\partial^2 u}{\partial t^2} \\
&k_7 w^{(4)} - k_6 \phi^{(3)} + \left[k_5 + \frac{1}{2}(2\mu_0 - \tau_0) T_p\right](-w'' + \phi') - \tau_0 S_P w'' = q - m_0 \frac{\partial^2 w}{\partial t^2} \\
&k_3 \phi^{(4)} + k_6 w^{(3)} - k_4 \phi'' + \left[k_5 + \frac{1}{2}(2\mu_0 - \tau_0) T_p\right](-w' + \phi) + (\lambda_0 + 2\mu_0) P_A u'' - (\lambda_0 + 2\mu_0) I_P \phi'' = f_\phi - m_2 \frac{\partial^2 \phi}{\partial t^2}
\end{aligned} \tag{67}$$

The boundary conditions can be written as

$$\begin{aligned}
&k_2 u' - k_1 u^{(3)} + N_s - \frac{1}{2}\tau_0 C_p = N_u^0 \quad \text{or} \quad u = \bar{u} \quad \text{at } x = 0 \quad \text{and} \quad x = L \\
&k_1 u'' = N_u^1 \quad \text{or} \quad u' = \bar{u}' \quad \text{at } x = 0 \quad \text{and} \quad x = L \qquad \frac{1}{2}Q_{s1} + \frac{1}{2}Q_{s2} + \tau_0 S_P w' = N_w^0 \quad \text{or} \quad w = \bar{w} \quad \text{at } x = 0 \quad \text{and} \quad x = L \\
&k_7 w'' - k_6 \phi' = N_w^1 \quad \text{or} \quad w' = \bar{w}' \quad \text{at } x = 0 \quad \text{and} \quad x = L \\
&k_4 \phi' - k_6 w'' - k_3 \phi^{(3)} - M_s + \frac{1}{2}\tau_0 P_A = N_\phi^0 \quad \text{or} \quad \phi = \bar{\phi} \quad \text{at } x = 0 \quad \text{and} \quad x = L \\
&k_3 = N_\phi^1 \quad \text{or} \quad \phi' = \bar{\phi}' \quad \text{at } x = 0 \quad \text{and} \quad x = L
\end{aligned} \tag{68}$$

where the overbar represents the prescribed value.

And the initial conditions can be written as

$$\left(m_0 \frac{\partial u}{\partial t}\delta u\right)\Bigg|_{t=0}^{t=T} = 0, \qquad \left(m_0 \frac{\partial w}{\partial t}\delta w\right)\Bigg|_{t=0}^{t=T} = 0,$$
$$\left(m_2 \frac{\partial \phi}{\partial t}\delta\phi\right)\Bigg|_{t=0}^{t=T} = 0 \tag{69}$$

Actually, the governing equations and boundary conditions of the new Timoshenko nanobeam model can degenerate into those of the new Bernoulli-Euler model if the shear deformation is ignored. Moreover, the new models can reduce to the corresponding models, in which size effects either only from the surface or only from the bulk are considered. These models can further reduce to the models that are based on the modified couple stress theory and the classical continuum theory. For clarity, the new models and the reduced models are summarized in Table 1. (Note: *CT*, *CS*, and *SG* represent the classical continuum model, the model based on modified couple stress theory, and the model based on strain gradient elasticity theory, respectively; *SE* represents surface effect.)

**Table 1.** References for Different Beam Models

| Different models | Bernoulli-Euler BEAM | | Timoshenko BEAM | |
|---|---|---|---|---|
| | Without SE | With SE | Without SE | With SE |
| CT | Dym and Shames (1973) | Chang and Rajapakse (2010) | Dym and Shames (1973) | Chang and Rajapakse (2010) |
| CS | Park and Gao (2006) | Gao and Mahmoud (2014) | Ma et al. (2008) | Gao (2015) |
| SG | Kong et al. (2009) | Present work | Wang et al. (2010) | Present work |

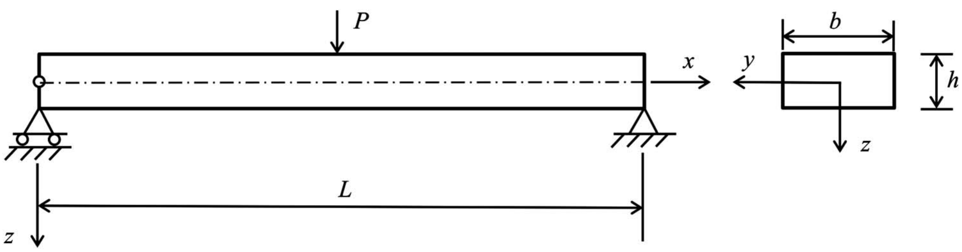


**Fig. 2.** Geometry and loading of a simply supported nanobeam



## Case Study for a Simply Supported Nanobeam

In order to illustrate the new size-dependent Bernoulli-Euler and Timoshenko nanobeam models developed in section "Formulation," the static bending and free vibration problems of a simply supported beam shown in Fig. 2 are solved in this section. For simplicity, axial deformation is not considered in the following examples. The simply supported beam is subject to a concentrated force at center point, and the geometrical parameters are given in Fig. 2. Unless otherwise indicated, the beam studied here is taken to be made of aluminum with the following properties (Liu and Rajapakse 2010): the elastic modulus $E = 90$ Gpa; the density $\rho = 2{,}700\ \mathrm{kg/m^3}$; Poisson's ratio $v = 0.23$; the material length scale parameter $l = 3$ nm; $l_0 = l_1 = l_2 = l$, $h_0 = 6$ nm; the thickness of the beam $h = k \cdot h_0$; $k$ is the dimensionless size scale; $b = 0.5h$; $L = 20h$; $P_0 = 1.0$ nN; the concentrated force $P = k \cdot P_0$; and the surface material properties are $\mu_0 = -5.4251$ N/m, $\lambda_0 = 3.4939$ N/m, and $\tau_0 = 0.5689$ N/m.

The boundary conditions of the static bending problem can be identified as (Ma et al. 2008)

$$u|_{x=0} = u|_{x=L} = 0, \qquad w|_{x=0} = w|_{x=L} = 0$$
$$w''|_{x=0} = w''|_{x=L} = 0, \qquad \phi'|_{x=0} = \phi'|_{x=L} = 0 \tag{70}$$

For a rectangular cross section with height $h$ and width $b$, using Eqs. (56), (58), and (60), the following can be achieved:

$$I = \frac{1}{12}bh^3, \qquad I_P = \frac{1}{6}h^3 + \frac{1}{2}bh^2, \qquad C_P = 2(b+h),$$
$$S_P = 2b, \qquad T_P = 2h, \qquad P_A = 0 \tag{71}$$

### Static Bending of Simply Supported Bernoulli-Euler Nanobeam

For the static bending problem, the time derivatives are set to zero in Eq. (36), then the governing equations for static problems are given by

$$Sw^{(4)} + (\lambda_0 + 2\mu_0)I_P w^{(4)} - Kw^{(6)} - \tau_0 S_P w'' - q = 0 \tag{72}$$

To derive the solutions, $w(x)$ can be expanded as the following Fourier series:

$$w(x) = \sum_{n=1}^{\infty} W_n^B \sin\left(\frac{n\pi x}{L}\right) \tag{73}$$

where $W_n^B$ = Fourier coefficients. It is clear that the expansions in Eq. (73) satisfy the boundary conditions in Eq. (70) for any $W_n^B$.

Based on Eq. (73), the applied load $q(x)$ can also be expanded in a Fourier series as

$$q(x) = \sum_{n=1}^{\infty} Q_n^B \sin\left(\frac{n\pi x}{L}\right) \tag{74}$$

For a given $q(x)$, $Q_n^B$ in Eq. (74) can be readily attained as

$$Q_n^B = \frac{2}{L}\int^L q(x)\sin\left(\frac{n\pi x}{L}\right)dx \tag{75}$$

For the present problem as shown in Fig. 2, $q(x) = P\delta(x - L/2)$, where $\delta(\cdot)$ is the Dirac delta function and $P$ is the concentrated force that has been given earlier. By substituting $q(x)$ of Eq. (74) into Eq. (75), it then leads to

$$Q_n^B = \frac{2}{L}P\sin\left(\frac{n\pi}{2}\right) \tag{76}$$

Substituting Eqs. (73) and (74) into Eq. (72), then, leads to

$$SW_n^B\left(\frac{n\pi}{L}\right)^4 + (\lambda_0 + 2\mu_0)I_P W_n^B\left(\frac{n\pi}{L}\right)^4 + KW_n^B\left(\frac{n\pi}{L}\right)^6 + \tau_0 S_p W_n^B\left(\frac{n\pi}{L}\right)^2 = Q_n^B \tag{77}$$

Solving the preceding linear equation [Eq. (77)], $W_n^B$ can be calculated as

$$W_n^B = \frac{Q_n^B}{S(\frac{n\pi}{L})^4 + (\lambda_0 + 2\mu_0)I_P(\frac{n\pi}{L})^4 + K(\frac{n\pi}{L})^6 + \tau_0 S_p(\frac{n\pi}{L})^2} \tag{78}$$

The analytical solutions of $w(x)$ for the static bending of the simply supported Bernoulli-Euler beam subjected to the concentrated force $P$ are determined by substituting Eq. (78) into Eq. (73).

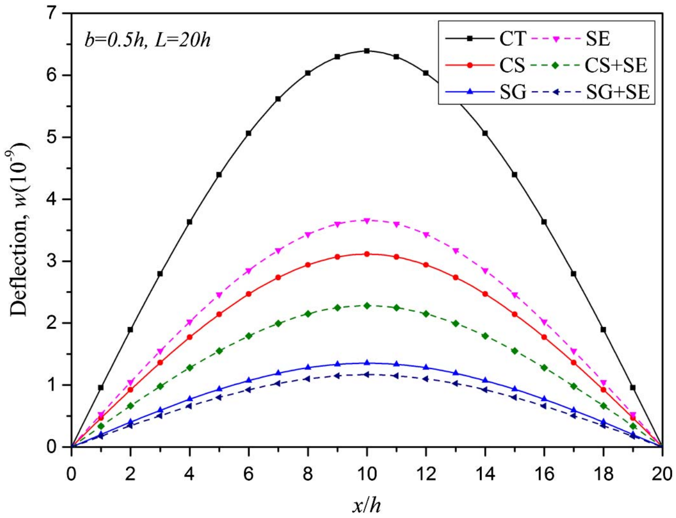


**Fig. 3.** Deflection of simply supported Timoshenko nanobeam based on different models

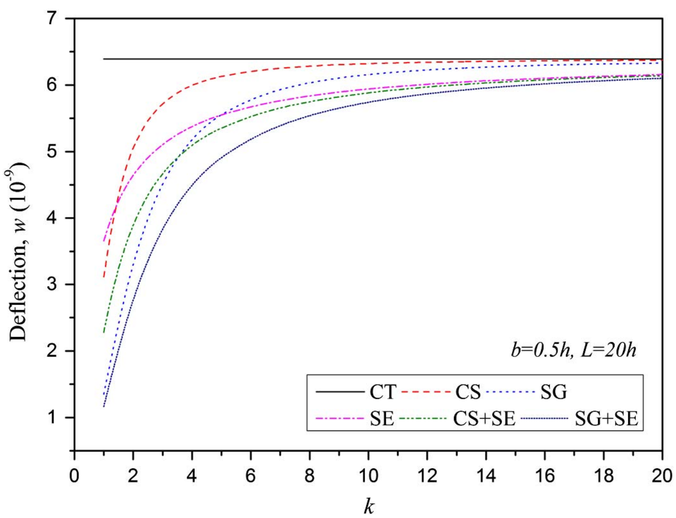


**Fig. 4.** Deflection varying with dimensionless size scale $k$

The deflection $w(x)$ of a Bernoulli-Euler beam is plotted in Fig. 3. Here, $k = 1$; the other parameters have been given earlier. From Fig. 3, it can be seen that the size effect is rather obvious. The deflection predicted by the present model is smaller than that predicted by the other five models. When the surface energy effects are considered, the deflection is smaller than that predicted by the corresponding models without considering surface energy effects.

Fig. 4 shows the variation of displacement of the simply supported Bernoulli-Euler beam with the size scale of the beam for different models. Here, the dimensionless size scale $k$ is the abscissa in Fig. 4, and the other parameters have been given earlier. For the classical model, the normalized stiffness remains unchanged as the size scale increases. And for the other five models, apart from the classical model, the normalized stiffness increases nonlinearly as the size scale increases. The differences between these models are reduced with the size scale increasing, while with a smaller size scale (i.e., smaller beam dimension for the same material), the present model shows strong size effect, and that leads to a higher normalized stiffness. Although the modified couple stress model and strain gradient model can also predict the size effect-induced increase of stiffness, the size-dependence is smaller than the present model. The couple stress theory considers the effect of the symmetric rotation gradient tensor, while the strain gradient theory considers the effects of the dilatation gradient tensor, the deviatoric stretch gradient tensor, and the symmetric rotation gradient tensor. Compared with the other models, the strain gradient theory model is more versatile because it is more physical. Fundamentally speaking, the increased stiffness predicted by the present model is contributed by the surface energy effects and the three strain gradient tensors of the strain gradient elasticity theory that underpins this model.

### Free Vibration of Simply Supported Bernoulli-Euler Nanobeam

Considering the free vibration problem of a simply supported Bernoulli-Euler beam shown in Fig. 2, all of the external force vanishes. Then the equation of motion of the beam satisfies

$$Sw^{(4)} + (\lambda_0 + 2\mu_0)I_P w^{(4)} - Kw^{(6)} - \tau_0 S_P w'' + m_0 \ddot{w} = 0 \quad (79)$$

Similar to the procedure of a static bending problem, $w(x)$ can be expanded as the following Fourier series:

$$w(x,t) = \sum_{n=1}^{\infty} W_n^V \sin\left(\frac{n\pi x}{L}\right) e^{i\omega_n t} \quad (80)$$

where $\omega_n$ = vibration frequency; $i$ = usual imaginary number; and $W_n^V$ = Fourier coefficient. Clearly, the expansion in Eq. (80) satisfies the boundary conditions in Eq. (70) for any $W_n^V$.

Substituting Eq. (80) into Eq. (79), then leads to

$$\left[S\left(\frac{n\pi}{L}\right)^4 + (\lambda_0 + 2\mu_0)I_P\left(\frac{n\pi}{L}\right)^4 + K\left(\frac{n\pi}{L}\right)^6 + \tau_0 S_P\left(\frac{n\pi}{L}\right)^2 - m_0\omega_n^2\right]W_n^V = 0 \quad (81)$$

For a nonzero solution of $W_n^V$, it is required that

$$S\left(\frac{n\pi}{L}\right)^4 + (\lambda_0 + 2\mu_0)I_P\left(\frac{n\pi}{L}\right)^4 + K\left(\frac{n\pi}{L}\right)^6 + \tau_0 S_P\left(\frac{n\pi}{L}\right)^2 - m_0\omega_n^2 = 0 \quad (82)$$

which leads to

$$\omega_n^2 = \frac{S(\frac{n\pi}{L})^4 + (\lambda_0 + 2\mu_0)I_P(\frac{n\pi}{L})^4 + K(\frac{n\pi}{L})^6 + \tau_0 S_P(\frac{n\pi}{L})^2}{m_0} \quad (83)$$

$\omega_n$ can be easily obtained:

$$\omega_n = \frac{\sqrt{S(\frac{n\pi}{L})^4 + (\lambda_0 + 2\mu_0)I_P(\frac{n\pi}{L})^4 + K(\frac{n\pi}{L})^6 + \tau_0 S_P(\frac{n\pi}{L})^2}}{\sqrt{m_0}} \quad (84)$$

Fig. 5 shows the change of the first order natural frequency of the simply supported Bernoulli-Euler beam predicted by six models with dimensionless thickness of the beam ($k$). From Fig. 5, it can be seen that the natural frequency predicted by the present model is larger than that predicted by the other five models. The results predicted by the models considering surface energy effects are larger than those predicted by the corresponding models neglecting surface energy effects. It is known that the higher frequency represents the higher stiffness, which results in the smaller deflection, so that shown in Fig. 5 is consistent with that shown in Fig. 4. With the

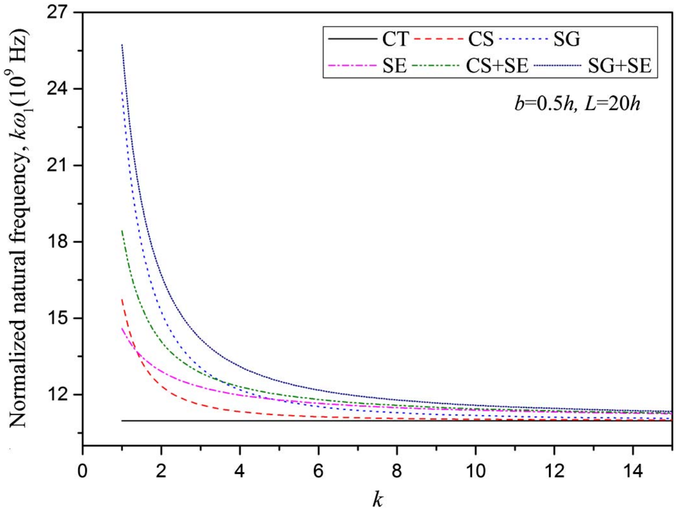


**Fig. 5.** Normalized natural frequency varying with size scale for different models

dimensionless size scale increasing, those differences gradually decrease. This illustrates that the size effect is prominent when the beam thickness is very small.

## Static Bending of Simply Supported Timoshenko Nanobeam

For the static bending problem, the time derivatives are set to zero in Eq. (67), the shear coefficient of Timoshenko beam $k_s$ is taken to be $(5+5v)/(6+5v)$, and for simplicity, the axial deformation is not considered here ($f_u = 0$), then the governing equations for static problems are given by

$$k_7 w^{(4)} - k_6 \phi^{(3)} + \left[k_5 + \frac{1}{2}(2\mu_0 - \tau_0)T_p\right](-w'' + \phi') - \tau_0 S_P = q$$

$$k_3 \phi^{(4)} + k_6 w^{(3)} - k_4 \phi'' + \left[k_5 + \frac{1}{2}(2\mu_0 - \tau_0)T_p\right] \times (-w' + \phi) + (\lambda_0 + 2\mu_0)P_A u'' - (\lambda_0 + 2\mu_0)I_P \phi'' = 0 \quad (85)$$

To derive the solutions, $w(x)$ and $\phi(x)$ can be expanded as the following Fourier series:

$$w(x) = \sum_{n=1}^{\infty} W_n^T \sin\left(\frac{n\pi x}{L}\right), \qquad \phi(x) = \sum_{n=1}^{\infty} \Phi_n^T \cos\left(\frac{n\pi x}{L}\right) \quad (86)$$

where $W_n^T$ and $\Phi_n^T$ = Fourier coefficients. It is clear that the expansions in Eq. (86) satisfy the boundary conditions in Eq. (70) for any $W_n^T$ and $\Phi_n^T$.

Based on Eq. (86), the applied load $q(x)$ can also be expanded in a Fourier series as

$$q(x) = \sum_{n=1}^{\infty} Q_n^T \sin\left(\frac{n\pi x}{L}\right) \quad (87)$$

For a given $q(x)$, $Q_n^T$ in Eq. (87) can be readily attained as

$$Q_n^T = \frac{2}{L}\int_L q(x)\sin\left(\frac{n\pi x}{L}\right)dx \quad (88)$$

For the present problem, $q(x) = P\delta(x - L/2)$, where $P$ = concentrated force, which has been given before and $\delta(\cdot)$ = Dirac delta function. By substituting $q(x)$ of Eq. (87) into Eq. (88), then it leads to

$$Q_n^T = \frac{2}{L}P\sin\left(\frac{n\pi}{2}\right) \quad (89)$$

Substituting Eqs. (86) and (87) into Eq. (85), then, leads to

$$\left\{k_7\left(\frac{n\pi}{L}\right)^2 + \left[k_5 + \frac{1}{2}(2\mu_0 - \tau_0)T_p\right] + \tau_0 S_P\right\}\left(\frac{n\pi}{L}\right)^2 W_n^T - \left\{k_6\left(\frac{n\pi}{L}\right)^2 + \left[k_5 + \frac{1}{2}(2\mu_0 - \tau_0)T_p\right]\right\}\frac{n\pi}{L}\Phi_n^T = Q_n^T$$

$$\left\{k_3\left(\frac{n\pi}{L}\right)^4 + k_4\left(\frac{n\pi}{L}\right)^2 + \left[k_5 + \frac{1}{2}(2\mu_0 - \tau_0)T_p\right] + (\lambda_0 + 2\mu_0)I_P\left(\frac{n\pi}{L}\right)^2\right\}\Phi_n^T - \left\{k_6\left(\frac{n\pi}{L}\right)^2 + \left[k_5 + \frac{1}{2}(2\mu_0 - \tau_0)T_p\right]\right\}\frac{n\pi}{L}W_n^T = 0 \quad (90)$$

Solving the linear equation [Eq. (90)], $W_n^T$ and $\Phi_n^T$ can be achieved:

$$W_n^T = \frac{\{k_3(\frac{n\pi}{L})^4 + k_4(\frac{n\pi}{L})^2 + [k_5 + \frac{1}{2}(2\mu_0 - \tau_0)T_p] + (\lambda_0 + 2\mu_0)I_P(\frac{n\pi}{L})^2\}Q_n^T}{\Delta}$$

$$\Phi_n^T = \frac{\{k_6(\frac{n\pi}{L})^2 + [k_5 + \frac{1}{2}(2\mu_0 - \tau_0)T_p]\}\frac{n\pi}{L}Q_n^T}{\Delta} \quad (91)$$

where

$$\Delta = \left\{k_7\left(\frac{n\pi}{L}\right)^2 + \left[k_5 + \frac{1}{2}(2\mu_0 - \tau_0)T_p\right] + \tau_0 S_P\right\}\left\{\left[k_3\left(\frac{n\pi}{L}\right)^2 + k_4 + (\lambda_0 + 2\mu_0)I_P\right]\left(\frac{n\pi}{L}\right)^2 + \left[k_5 + \frac{1}{2}(2\mu_0 - \tau_0)T_p\right]\right\}\left(\frac{n\pi}{L}\right)^2 - \left\{k_6\left(\frac{n\pi}{L}\right)^2 + \left[k_5 + \frac{1}{2}(2\mu_0 - \tau_0)T_p\right]\right\}\left\{k_6\left(\frac{n\pi}{L}\right)^2 + \left[k_5 + \frac{1}{2}(2\mu_0 - \tau_0)T_p\right]\right\}\left(\frac{n\pi}{L}\right)^2 \quad (92)$$

The analytical solutions of $w(x)$ and $\phi(x)$ for the static bending of the simply supported Timoshenko beam subjected to the concentrated force $P$ are determined by using Eqs. (86), (91), and (92).

Using the newly developed Timoshenko beam model, the static bending problem of a simply supported Timoshenko beam is investigated. Here, $k = 1$, and for simplicity, parameters have been given earlier. Figs. 6 and 7 show the deflection and the corresponding

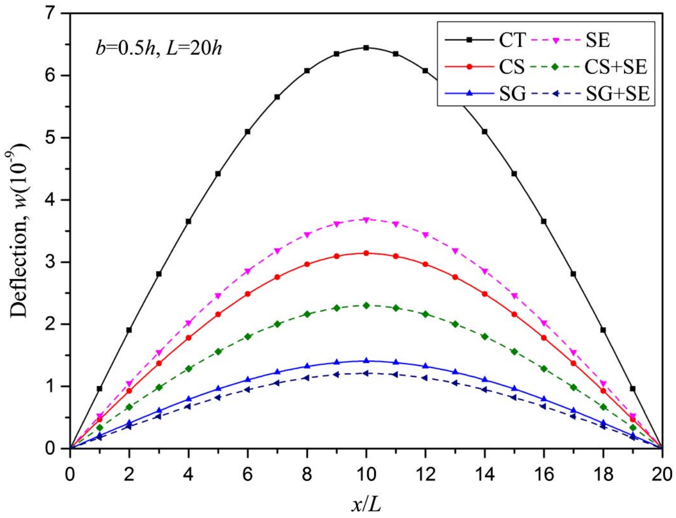


**Fig. 6.** Deflection of simply supported Timoshenko beam

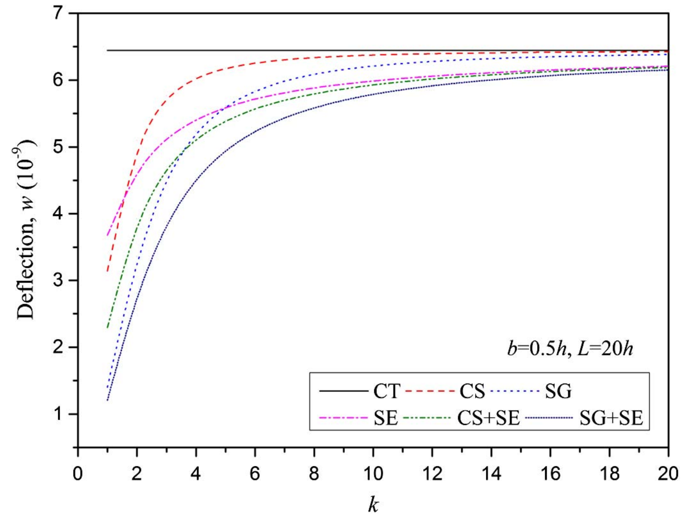


**Fig. 8.** Deflection varying with dimensionless size scale

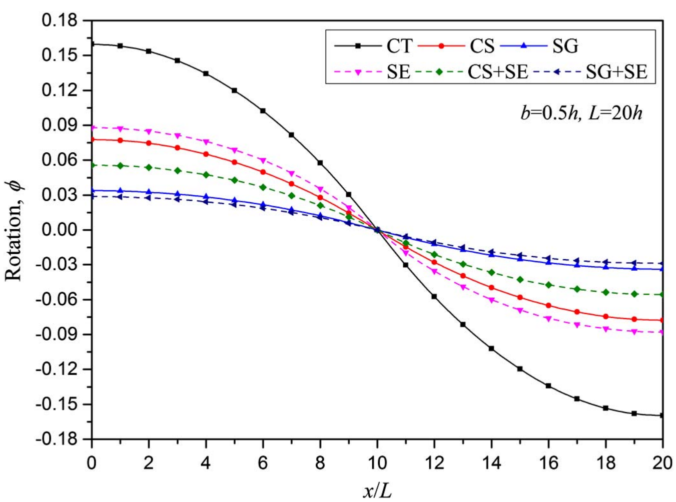


**Fig. 7.** Rotation of simply supported Timoshenko beam

rotation of the simply supported Timoshenko beam, respectively. It can be clearly observed that the deflection predicted by the present model is smaller than that of the other five models. The absolute values of the rotation of the simply supported Timoshenko beam predicted by three models in Fig. 7, show the similar trend as shown in Fig. 6.

Fig. 8 shows the variation of displacement of the simply supported Timoshenko beam with the dimensionless size scale of the beam. For the classical model, the normalized stiffness remains unchanged as the size scale increases. And for the other five models, apart from the classical model, the normalized stiffness increases nonlinearly as the size scale increases. The differences between these models reduce with the size scale increasing, while with a smaller size scale the present model shows strong size effect, and that leads to a higher normalized stiffness. Although the modified couple stress model and strain gradient model can also predict the size effect-induced increase of stiffness, the size-dependence is smaller than the present model. Compared to the modified couple stress theory, the strain gradient elasticity theory introduces additional dilatation gradient tensor and the deviatoric stretch gradient tensor in addition to the symmetric rotation gradient tensor. So the strain gradient theory is more versatile. Fundamentally speaking, the increased stiffness predicted by the present model is contributed by the surface energy effects and the three strain gradient tensors of the strain gradient elasticity theory that underpins this model.

### Free Vibration of Simply Supported Timoshenko Nanobeam

Considering the free vibration problem of a simply supported Timoshenko beam shown in Fig. 2, all of the external force vanishes. Then the equations of motion of the beam satisfies

$$
\begin{aligned}
&k_7 w^{(4)} - k_6\phi^{(3)} + \left[k_5 + \frac{1}{2}(2\mu_0 - \tau_0)T_p\right](-w'' + \phi') - \tau_0 S_P w'' \\
&\quad = -m_0\frac{\partial^2 w}{\partial t^2} \\
&k_3\phi^{(4)} + k_6 w^{(3)} - k_4\phi'' + \left[k_5 + \frac{1}{2}(2\mu_0 - \tau_0)T_p\right](-w' + \phi) \\
&\quad + (\lambda_0 + 2\mu_0)P_A u'' - (\lambda_0 + 2\mu_0)I_P\phi'' = -m_2\frac{\partial^2\phi}{\partial t^2}
\end{aligned}
\tag{93}
$$

Similar to the procedure of the static bending problem, $w(x)$ and $\phi(x)$ can be expanded as the following Fourier series:

$$
\begin{aligned}
w(x,t) &= \sum_{n=1}^{\infty} W_n^D \sin\left(\frac{n\pi x}{L}\right)e^{i\omega_n t}, \\
\phi(x,t) &= \sum_{n=1}^{\infty} \Phi_n^D \cos\left(\frac{n\pi x}{L}\right)e^{i\omega_n t}
\end{aligned}
\tag{94}
$$

where $\omega_n$ = vibration frequency; $i$ = usual imaginary number; $W_n^D$ and $\Phi_n^D$ = Fourier coefficients. Clearly, the expansions in Eq. (94) satisfy the boundary conditions in Eq. (70) for any $W_n^D$ and $\Phi_n^D$.

Substituting Eq. (94) into Eq. (93), then leads to

$$
\begin{bmatrix} a_1 & a_2 \\ a_3 & a_4 \end{bmatrix}\begin{Bmatrix} W_n^D \\ \Phi_n^D \end{Bmatrix} = 0 \tag{95}
$$

where

$$a_1 = k_7\left(\frac{n\pi}{L}\right)^4 + \left[k_5 + \frac{1}{2}(2\mu_0 - \tau_0)T_p\right]\left(\frac{n\pi}{L}\right)^2 + \tau_0 S_P\left(\frac{n\pi}{L}\right)^2 - m_0\omega_n^2$$
$$a_2 = -\left\{k_6\left(\frac{n\pi}{L}\right)^2 + \left[k_5 + \frac{1}{2}(2\mu_0 - \tau_0)T_p\right]\right\}\frac{n\pi}{L}$$
$$a_3 = -\left\{k_6\left(\frac{n\pi}{L}\right)^2 + \left[k_5 + \frac{1}{2}(2\mu_0 - \tau_0)T_p\right]\right\}\frac{n\pi}{L}$$
$$a_4 = k_3\left(\frac{n\pi}{L}\right)^4 + k_4\left(\frac{n\pi}{L}\right)^2 + \left[k_5 + \frac{1}{2}(2\mu_0 - \tau_0)T_p\right] + (\lambda_0 + 2\mu_0)I_P\left(\frac{n\pi}{L}\right)^2 - m_2\omega_n^2 \quad (96)$$

For a nonzero solution of $W_n^D$ and $\Phi_n^D$, it is required that the determinant of the coefficients matrix of Eq. (95) vanishes, which leads to

$$e_1\omega_n^4 + e_2\omega_n^2 + e_3 = 0 \quad (97)$$

where

$$e_1 = m_0 m_2$$
$$e_2 = -\left\{k_7\left(\frac{n\pi}{L}\right)^4 + \left[k_5 + \frac{1}{2}(2\mu_0 - \tau_0)T_p\right]\left(\frac{n\pi}{L}\right)^2 + \tau_0 S_P\left(\frac{n\pi}{L}\right)^2\right\}m_2 - m_0\left\{k_3\left(\frac{n\pi}{L}\right)^4 + k_4\left(\frac{n\pi}{L}\right)^2 + \left[k_5 + \frac{1}{2}(2\mu_0 - \tau_0)T_p\right] + (\lambda_0 + 2\mu_0)I_P\left(\frac{n\pi}{L}\right)^2\right\}$$
$$e_3 = \left\{k_7\left(\frac{n\pi}{L}\right)^4 + \left[k_5 + \frac{1}{2}(2\mu_0 - \tau_0)T_p\right]\left(\frac{n\pi}{L}\right)^2 + \tau_0 S_P\left(\frac{n\pi}{L}\right)^2\right\}\left\{k_3\left(\frac{n\pi}{L}\right)^4 + k_4\left(\frac{n\pi}{L}\right)^2 + \left[k_5 + \frac{1}{2}(2\mu_0 - \tau_0)T_p\right] + (\lambda_0 + 2\mu_0)I_P\left(\frac{n\pi}{L}\right)^2\right\} - \left\{k_6\left(\frac{n\pi}{L}\right)^2 + \left[k_5 + \frac{1}{2}(2\mu_0 - \tau_0)T_p\right]\right\}^2\left(\frac{n\pi}{L}\right)^2 \quad (98)$$

The equation of $\omega_n^2$ can be easily obtained by solving the quadratic equation [Eq. (97)]:

$$\omega_n^2 = \frac{-e_2 - \sqrt{e_2^2 - 4e_1e_3}}{2e_1} \quad (99)$$

Fig. 9 shows the change of the first order natural frequency of the simply supported Timoshenko beam predicted by different models with the dimensionless size scale of the beam. From Fig. 9, it can be seen that the natural frequency predicted by the present model is larger than that predicted by the other five models. The results predicted by the models considering surface energy effects are larger than those predicted by the corresponding models neglecting surface energy effects. The higher frequency represents the higher stiffness, which results in the smaller deflection, so that shown in Fig. 9 is consistent with that shown in Fig. 8. With the dimensionless thickness increasing, those differences gradually decrease, which illustrates that the size effect is prominent when the beam thickness is very small.

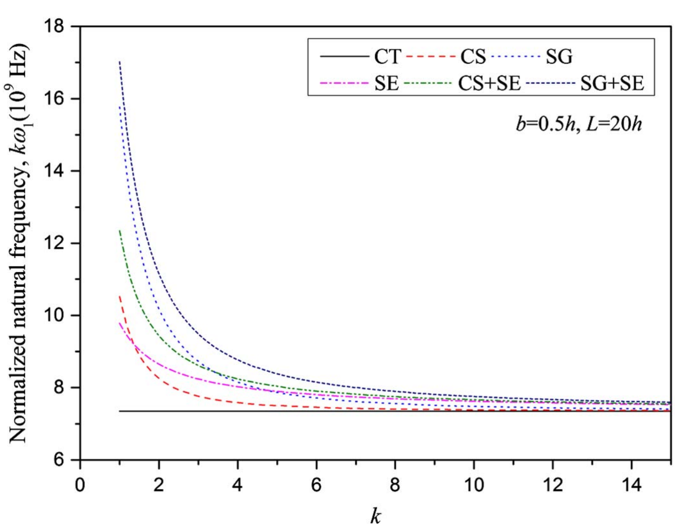


**Fig. 9.** Normalized natural frequency varying with dimensionless size scale for different models

## Conclusions

With size effect originating from the surface and bulk included, the size-dependent nanoscale Bernoulli-Euler and Timoshenko beam models are developed based on surface elasticity theory and strain gradient elasticity theory by a variational method. The new models, containing three material length scale parameters and three surface elasticity constants, can capture the size effect in the bulk and surface layer of the beam. These two models recover the models considering only the microstructure dependence or the surface energy effect. And these two models also can degenerate into the modified couple stress models or the classical models as limiting cases. In addition, the new Timoshenko beam model recovers the new Bernoulli-Euler beam when shear deformation is ignored. The static bending and free vibration problems of a simply supported nanoscale Bernoulli-Euler beam and Timoshenko beam are solved respectively to illustrate the new models. Numerical results reveal that the differences in the deflection, rotation, and natural frequency predicted by the present model and the other models are large when the size of the beam is small. These differences, however, are decreasing or even diminishing with the increase of the size of the beam.

## Acknowledgments

The work is supported by the National Natural Science Foundation of China (Grant No. 11202117, 51422904, 51379112, and 11272186), Natural Science Fund of Shandong Province (BS2012ZZ006), and the Fundamental Research Funds of Shandong University (Grant No. 2015JX003).

## References


Asghari, M., Ahmadian, M. T., Kahrobaiyan, M. H., and Rahaeifard, M. (2010a). "On the size-dependent behavior of functionally graded micro-beams." *Mater. Des.*, 31(5), 2324–2329.

Asghari, M., Kahrobaiyan, M. H., and Ahmadian, M. T. (2010b). "A nonlinear Timoshenko beam formulation based on the modified couple stress theory." *Int. J. Eng. Sci.*, 48(12), 1749–1761.

Asghari, M., Rahaeifard, M., Kahrobaiyan, M. H., and Ahmadian, M. T. (2011). "The modified couple stress functionally graded Timoshenko beam formulation." *Mater. Des.*, 32(3), 1435–1443.

Chang, L., and Rajapakse, R. K. N. D. (2010). "Continuum models incorporating surface energy for static and dynamic response of nanoscale beams." *IEEE Trans. on Nanotechnol.*, 9(4), 422–431.

Chasiotis, I., and Knauss, W. G. (2003). "The mechanical strength of polysilicon films. Part 2: Size effects associated with elliptical and circular perforations." *J. Mech. Phys. Solids*, 51(8), 1551–1572.

Dym, C. L., and Shames, I. H. (1973). *Solid mechanics: A variational approach*, McGraw-Hill, New York.

Eringen, A. C. (1983). "On differential-equations of nonlocal elasticity and solutions of screw dislocation and surface-waves." *J. Appl. Phys.*, 54(9), 4703–4710.

Fathalilou, M., Sadeghi, M., and Rezazadeh, G. (2014). "Micro-inertia effects on the dynamic characteristics of micro-beams considering the couple stress theory." *Mech. Res. Commun.*, 60, 74–80.

Gao, X. L. (2015). "A new Timoshenko beam model incorporating microstructure and surface energy effects." *Acta Mech.*, 226(2), 457–474.

Gao, X. L., and Mahmoud, F. F. (2014). "A new Bernoulli-Euler beam model incorporating microstructure and surface energy effects." *Z. Angew. Math. Phys.*, 65(2), 393–404.

Gurtin, M. E., and Murdoch, A. I. (1975). "A continuum theory of elastic material surfaces." *Archiv. Ration. Mech. Anal.*, 57(4), 291–323.

Gurtin, M. E., and Murdoch, A. I. (1978). "Surface stress in solids." *Int. J. Solids Struct.*, 14(6), 431–440.

Jiang, L. Y., and Yan, Z. (2010). "Timoshenko beam model for static bending of nanowires with surface effects." *Phys. E: Low-dimensional Syst. Nanostruct.*, 42(9), 2274–2279.

Koiter, W. T. (1964). "Couple stresses in the theory of elasticity, I and II." *Proc. Koninkl. Ned. Akad. Wet.*, 67, 17–44.

Kong, S., Zhou, S., Nie, Z., and Wang, K. (2009). "Static and dynamic analysis of micro beams based on strain gradient elasticity theory." *Int. J. Eng. Sci.*, 47(4), 487–498.

Koochi, A., Hosseini-Toudeshky, H., Ovesy, H. R., and Abadyan, M. (2013). "Modeling the influence of surface effect on instability of nano-cantilever in presence of van der Waals force." *Int. J. Struct. Stab. Dyn.*, 13(4), 1250072.

Lam, D. C. C., and Chong, A. C. M. (1999). "Indentation model and strain gradient plasticity law for glassy polymers." *J. Mater. Res.*, 14(9), 3784–3788.

Lam, D. C. C., Yang, F., Chong, A. C. M., Wang, J., and Tong, P. (2003). "Experiments and theory in strain gradient elasticity." *J. Mech. Phys. Solids*, 51(8), 1477–1508.

Liang, B., Zhang, L., Wang, B., and Zhou, S. (2015). "A variational size-dependent model for electrostatically actuated NEMS incorporating nonlinearities and Casimir force." *Phys. E: Low-dimensional Syst. Nanostruct.*, 71, 21–30.

Liu, C., and Rajapakse, R. (2010). "Continuum models incorporating surface energy for static and dynamic response of nanoscale beams." *IEEE Trans. Nanotechnol.*, 9(4), 422–431.

Ma, H. M., Gao, X. L., and Reddy, J. N. (2008). "A microstructure-dependent Timoshenko beam model based on a modified couple stress theory." *J. Mech. Phys. Solids*, 56(12), 3379–3391.

McFarland, A. W., and Colton, J. S. (2005). "Role of material microstructure in plate stiffness with relevance to microcantilever sensors." *J. Micromech. Microeng.*, 15(5), 1060–1067.

Park, S. K., and Gao, X. L. (2006). "Bernoulli-Euler beam model based on a modified couple stress theory." *J. Micromech. Microeng.*, 16(11), 2355–2359.

Poole, W. J., Ashby, M. F., and Fleck, N. A. (1996). "Micro-hardness of annealed and work-hardened copper polycrystals." *Scr. Mater.*, 34(4), 559–564.

Sadeghian, H., Goosen, H., Bossche, A., Thijsse, B., and van Keulen, F. (2011). "On the size-dependent elasticity of silicon nanocantilevers: Impact of defects." *J. Phys. D-Appl. Phys.*, 44(7), 072001.

Shaat, M., Mahmoud, F. F., Gao, X. L., and Faheem, A. F. (2014). "Size-dependent bending analysis of Kirchhoff nano-plates based on a modified couple-stress theory including surface effects." *Int. J. Mech. Sci.*, 79, 31–37.

Shenoy, V. B. (2005). "Atomistic calculations of elastic properties of metallic fcc crystal surfaces." *Phys. Rev. B*, 71(9), 094104.

Tsiatas, G. C. (2009). "A new Kirchhoff plate model based on a modified couple stress theory." *Int. J. Solids Struct.*, 46(13), 2757–2764.

Vardoulakis, I., Exadaktylos, G., and Kourkoulis, S. K. (1998). "Bending of marble with intrinsic length scales: A gradient theory with surface energy and size effects." *Journal de physique. IV (Les Ulis)*, 8(8), 399–406.

Wang, B., Liu, M., Zhao, J., and Zhou, S. (2014). "A size-dependent Reddy-Levinson beam model based on a strain gradient elasticity theory." *Meccanica*, 49(6), 1427–1441.

Wang, B., Zhao, J., and Zhou, S. (2010). "A micro scale Timoshenko beam model based on strain gradient elasticity theory." *Eur. J. Mech.-A/Solids*, 29(4), 591–599.

Wang, B., Zhao, J., Zhou, S., and Chen, X. (2011a). "A size-dependent Kirchhoff micro-plate model based on strain gradient elasticity theory." *Eur. J. Mech.- A/Solids*, 30(4), 517–524.

Wang, B., Zhou, S., Zhao, J., and Chen, X. (2012). "Pull-in instability of circular plate MEMS: A new model based on strain gradient elasticity theory." *Int. J. Appl. Mech.*, 4(1), 1250003.

Wang, B. L., Zhou, S. J., Zhao, J. F., and Chen, X. (2011c). "Size-dependent pull-in instability of electrostatically actuated microbeam-based MEMS." *J. Micromech. Microeng.*, 21(2), 027001.

Xia, W., Wang, L., and Yin, L. (2010). "Nonlinear non-classical microscale beams: Static bending, postbuckling, and free vibration." *Int. J. Eng. Sci.*, 48(12), 2044–2053.

Yang, F., Chong, A. C. M., Lam, D. C. C., and Tong, P. (2002). "Couple stress based strain gradient theory for elasticity." *Int. J. Solids Struct.*, 39(10), 2731–2743.

Yin, L., Qian, Q., and Wang, L. (2011). "Size effect on the static behavior of electrostatically actuated microbeams." *Acta Mech. Sin.*, 27(3), 445–451.

Zhao, J. G., Zhou, S. J., Wang, B. L., and Wang, X. P. (2012). "Nonlinear microbeam model based on strain gradient theory." *Appl. Math. Model.*, 36(6), 2674–2686.